

1 **LAESI mass spectrometry imaging as a tool to differentiate the root**
2 **metabolome of native and range-expanding plant species**

3 Purva Kulkarni*, Rutger A. Wilschut, Koen J.F. Verhoeven, Wim H. van der Putten and Paolina

4 Garbeva

5 Netherlands Institute of Ecology (NIOO-KNAW), Droevendaalsesteeg 10, 6708 PB Wageningen, The

6 Netherlands

7 ***Corresponding author:** Purva Kulkarni

8 Tel.: +31 (0)317 473 511

9 Email: P.Kulkarni@nioo.knaw.nl

10 **Email address of co-authors:**

11 Rutger A. Wilschut - R.Wilschut@nioo.knaw.nl

12 Koen J.F. Verhoeven - K.Verhoeven@nioo.knaw.nl

13 Wim H. van der Putten - <mailto:W.vanderPutten@nioo.knaw.nl>

14 Paolina Garbeva - P.Garbeva@nioo.knaw.nl

15 **ABSTRACT**

16 Our understanding of chemical diversity in biological samples has greatly improved through recent
17 advances in mass spectrometry (MS). MS-based-imaging (MSI) techniques have further enhanced
18 this by providing spatial information on the distribution of metabolites and their relative abundance.

19 This study aims to employ laser-assisted electrospray ionization (LAESI) MSI as a tool to profile and
20 compare the root metabolome of two pairs of native and range expanding plant species.

21 It has been proposed that successful range-expanding plant species, like introduced exotic invaders,
22 have a novel, or a more diverse secondary chemistry. Although some tests have been made using
23 aboveground plant materials, tests using root materials are rare. We tested the hypothesis that range-
24 expanding plants possess more diverse root chemistries than native plant species.

25 To examine the root chemistry of the selected plant species, LAESI-MSI was performed in positive ion
26 mode and data was acquired in a mass range of m/z 50-1200 with a spatial resolution of 100 μm . The

27 acquired data was analyzed using in-house scripts, and differences in the spatial profiles were studied
28 for discriminatory mass features.

29 The results revealed clear differences in the metabolite profiles amongst and within both pairs of
30 congeneric plant species, in the form of distinct metabolic fingerprints. The use of ambient conditions
31 and the fact that no sample preparation was required, established LAESI-MSI as an ideal technique
32 for untargeted metabolomics and for direct correlation of the acquired data to the underlying
33 metabolomic complexity present in intact plant samples.

34 **KEYWORDS**

35 Mass spectrometry imaging, LAESI, ambient imaging, metabolomics, root metabolome, data analysis,
36 metabolic profiling

37 **BACKGROUND**

38 Detection of plant metabolites is extremely challenging, as there is no single-instrument platform
39 available to effectively measure their overall coverage. During the last decade, mass spectrometry
40 imaging (MSI) has emerged as a valuable tool, with numerous applications in the field of biological
41 sciences. This analytical technique enables label-free, high-resolution spatial mapping of a large
42 variety of biomolecules along with providing qualitative and quantitative chemical information, in a
43 single experiment [1]. Identical to traditional mass spectrometry, during MSI it is important to ionize the
44 sample to form ions suitable for mass analysis. Different ionization methods exist for MSI, however
45 many of them require artificially altering the biochemical status of the system under study, for example
46 by the use of a matrix, and are mainly operated under vacuum. Recently developed ambient ionization
47 approaches such as laser ablation electrospray ionization (LAESI) allow direct analysis of biological
48 samples in a matrix-free, native atmospheric condition with minimal to no sample preparation [2,3].
49 This opens up possibilities for in situ chemical analysis in biological systems.

50 LAESI-MSI is particularly tailored for biological samples that are rich in water content [4]. In
51 this technique, the sample under investigation is mounted on a sample stage and is ablated using a
52 focused mid-Infrared laser pulse, under atmospheric conditions. This ablation ejects a mixture of
53 molecules, clusters, and particulate matter in microscopic volumes from the sample, in the form of a
54 plume. The catapulted biomolecules then coalesce with charged droplets, produced by an

55 electrospray to become ionized [5,6]. MSI using the LAESI ionization approach is realized by rastering
56 the sample surface at pre-defined coordinates with a laser beam, where at each coordinate position
57 the generated ions pass through the mass analyzer and a mass spectrum is recorded. LAESI-MSI has
58 shown considerable success in revealing the lateral and cross-sectional distribution of primary and
59 secondary metabolites for a range of plant related samples, along with providing chemical information
60 from deeper parts of the tissue section [7]. LAESI equipped with a sharpened optical fiber tip has also
61 been widely used to perform in situ metabolic profiling of single cells from plant and animal samples
62 [8].

63 Here, we aim to demonstrate the potential of LAESI-MSI as an analytical technique for the direct
64 metabolite profiling of plant samples. We applied LAESI-MSI in a comparative metabolic profiling study
65 on two pairs of non-native, range-expanding plant species and congeneric native plant species. In
66 response to recent climate warming, many plant species have expanded their range to higher latitudes
67 and altitudes [9,10]. It is thought that plant secondary chemistry is an important factor determining the
68 invasive success of exotic plant species. The novel chemistry of invasive exotic plant species may
69 effectively control defenses against insect herbivores and other natural enemies [11]. Such 'novel
70 chemistry' has been shown to potentially suppress native plant species directly through allelopathy
71 [12] or indirectly through the suppression of the fungal mutualists of native plant species [13,14].
72 Moreover, due to this difference in chemistry, native generalist herbivores may perform less well on
73 exotic plant species than on related native plant species [15], potentially leading to a reduced
74 herbivore pressure on exotics compared to natives. The poor performance of generalist herbivores
75 has also been linked to the high diversity of metabolites produced by exotic plant species compared to
76 native plant species [16]. This suggests that chemically diverse plant species may be prone to become
77 abundant when they are introduced in a new area where the local herbivores are poorly adapted to
78 neutralize, or circumvent the novel defenses.

79 In this study, we use LAESI-MSI as a high-throughput tool for untargeted comparative metabolomics
80 of intact plant roots of native and range expanding plant species. For this, we use two range-
81 expanding plant species that are currently expanding in North-Western Europe, *Centaurea stoebe* L.
82 and *Geranium pyrenaicum* Burm. f., and their respective congeneric native species *Centaurea jacea* L.
83 and *Geranium molle* L. With this study, we demonstrate the suitability of LAESI-MSI for untargeted

84 metabolomics profiling and we give insights in the potential chemical novelty of range-expanding plant
85 species in comparison to congeneric related native plant species.

86 DATA DESCRIPTION

87 In order to perform untargeted comparative root metabolomics using LAESI-MSI, two pairs of native
88 plant species and their respective range-expanding species were selected. Intact root samples were
89 collected from three biological replicates for the native species *Centaurea jacea* L. and *Geranium*
90 *molle* L and their respective range expanding plant species *Centaurea stoebe* L. and *Geranium*
91 *pyrenaicum* Burm. f. These twelve intact root samples were mounted on the sample stage one-by-one
92 to perform LAESI-MSI in positive ion mode. The mass spectral data was acquired in a mass range of
93 m/z 50-1200 from 105 pre-defined coordinate positions (spots) present on each sample replicate. The
94 acquired data was first lock-mass corrected using an internal standard. Since all the 105 LAESI
95 ablation spots for a single replicate were not present on the root sample, mass spectra arising from
96 only 50 spots per replicate, that were visibly present on the root sample were selected manually.
97 These extracted mass spectra were subjected to multiple data preprocessing steps. After performing
98 peak detection on the preprocessed data, a mass feature matrix was generated. Multivariate data
99 analysis was performed on the feature matrix to screen out significant differentially expressed
100 metabolites amongst the samples.

101 ANALYSES

102 Untargeted metabolite profiling and multivariate analysis

103 Untargeted metabolomic studies are exploratory in nature and usually result in extremely large and
104 multi-dimensional datasets. Analyses of such datasets using chemometric tools can hugely aid data
105 interpretation.

106 The representative averaged preprocessed spectra for each replicate belonging to the different plant
107 species show a clear distinction in mass spectra between the two plant genera (**Figure 1**). This
108 distinction between *Centaurea* and *Geranium* samples was confirmed by unsupervised hierarchical
109 clustering of the mass feature matrix (**Figure 2a**). Within the two genera, the different plant species
110 were mostly clearly separated based on their chemical features, with the exception of one of the *C.*
111 *stoebe* replicates (**Figure 2a**).

112 Visual comparison of the representative mass spectrum for each sample group can be used to broadly
113 study the differing metabolic profiles. To further examine these differences and similarities between
114 the root metabolic profiles of the four plant species, we employed PCA. The first two selected principal
115 component axes explain over 75% of cumulative variance amongst the samples (**Figure 2b**). Samples
116 from different plant genera were strongly separated along the first PC-axis (~57%), whereas the
117 separation along the second PC-axis (~18%) corresponded with within-genus variation (**Figure 2b**).
118 Together with hierarchical clustering (**Figure 2a**), these results indicate a strong phylogenetic signal in
119 root chemistry, as between-genus variation is considerably stronger than within-genus variation [17].

120 The number of mass features detected for each LAESI-MSI acquisition after performing data
121 pre-processing and peak-detection clearly shows that there are more mass features detected for the
122 replicates of *Centaurea* as compared to those of *Geranium* (**Table 1**). The two *Centaurea* species
123 shared 314 metabolites, whereas 53 metabolites were unique to either one of the species (**Figure 3**
124 **a**). Interestingly, 49 of these metabolites were unique for range-expanding *C. stoebe*, whereas only 4
125 were unique for native *C. jacea*. In contrast, for native *G. molle* more unique metabolites were
126 detected than in range-expanding *G. pyrenaicum* (**Figure 3b**). These results are in line with a previous
127 study in which only root volatiles were examined [18] and indicate that range-expanding plants do not
128 necessarily possess a more unique root chemistry than related natives.

129 In order to visualize the statistically significant metabolites for the two *Centaurea* species, a
130 volcano plot was constructed (**Figure 4a**). As can be seen in **Figure 4a**, in total 367 metabolites were
131 detected in genus *Centaurea*. Within this, 10 mass features (shown in green) that are located in upper
132 right quadrant of the plot, indicate that their concentration is significantly higher in native species *C.*
133 *jacea* than in range expanding species *C. stoebe*. The 5 mass features (shown in red) that are
134 observed in the upper left quadrant indicate that their concentration is significantly lower in native
135 species *C. jacea* than in range expanding species *C. stoebe*. To examine the differences in metabolite
136 concentrations for the *C. jacea* and *C. stoebe* pair, box-and-whisker plots were realized for four
137 statistically significant metabolites chosen based on the volcano plot (**Figure 4b**). As can be seen in
138 box-and-whisker plots and the ion intensity maps, *m/z* 84.9607, *m/z* 159.0520 and *m/z* 557.290 are
139 highly abundant in native species *C. jacea*, whereas *m/z* 272.9550 are highly abundant in range-
140 expanding species *C. stoebe*. Additionally, the corresponding ion intensity maps for these metabolites
141 were also generated to visualize the changes on the spatial level in the imaged roots. The ion intensity

142 maps can be seen alongside the box-and-whisker plots in **Figure 4b**. Each ion map is plotted on the
143 same color scale (depicted below the ion maps) ranging from 0 (blue meaning least intense) to 1 (red
144 meaning most intense), to allow comparison of relative ion intensity between images.

145 Similar analysis was performed for the two *Geranium* species (**Figure 4c**). For this pair, in
146 total 175 metabolites were detected. Within these, 15 mass features (shown in green) that are located
147 in the upper right quadrant of the plot, which indicates that their concentrations are significantly higher
148 in native species *G. molle* than in range expanding species *G. pyrenaicum*. The 4 mass features
149 (shown in red) that are observed in the upper left quadrant indicates that their concentration is
150 significantly lower in native species *G. molle* than in range expanding species *G. pyrenaicum*. The
151 box-and-whisker plots for the four statistically significant metabolites selected from the volcano plot for
152 the pair *G. molle* and *G. pyrenaicum* are shown in **Figure 4d**. The ion intensity maps for these
153 statistically significant metabolites are shown alongside box-and-whisker plots. As can be seen, *m/z*
154 158.2647 and *m/z* 250.8271 show high abundance in native species *G. molle*, whereas *m/z* 172.3829
155 and *m/z* 196.5855 display high abundance in range expanding species *G. pyrenaicum*. All significant
156 metabolites detected for *Centaurea* and *Geranium* samples are listed in **Supplementary Table 1**.

157 **DISCUSSION**

158 In this study, we demonstrated the utility of the ambient ionization ability of LAESI coupled with MSI to
159 explore the chemical differences in the root metabolome between two pairs of native and range
160 expanding plant species. This high-throughput technology provided an *in situ* analysis method capable
161 of revealing differentially produced metabolites linked to each group. We detected clear differences in
162 root chemical profiles within both pairs of range-expanding plant species and congeneric natives using
163 untargeted LAESI-MSI approach. Interestingly, the range-expanding plant species *Centaurea stoebe*
164 showed a strongly unique root chemistry, which also may have enabled this species to become
165 invasive in its introduced range in North America [15,19].

166 Furthermore we demonstrated that LAESI-MSI can help to spatially elucidate the metabolite
167 composition of the intact roots with minimal to no sample preparation. Our demonstration did not
168 involve an exhaustive region-specific spatial analysis of the roots, but rather a 'proof of concept' by
169 lateral profiling of the root samples. This allowed us to establish that LAESI-MSI of whole-root sections
170 could reveal information on location-specific metabolite distribution without the need for any sample

171 preparation. These results can help to reveal the role of single metabolites based on their location
172 within the roots.

173 Overall, our results illustrate the feasibility of LAESI–MSI as a high-throughput technique for the
174 detection and localization of metabolites from intact plant samples and gaining spatial information
175 without the need for extensive sample preparation. The potential applications of this work could lead to
176 rapid phenotyping of plant tissues as well as comparative untargeted metabolomics of different plant
177 parts, a topic of considerable recent interest for plant research.

178 **METHODS**

179 **Plant species and root collection**

180 The seeds used for all four plant species originated from natural populations in natural areas in The
181 Netherlands, where the range expanders are immigrating. Seeds of *G. molle* and *C. stoebe* were
182 collected directly from the field. For *C. jacea*, seeds were collected from plants growing in an
183 experimental garden, whereas the mother plants were germinated from field-collected seeds. Seed
184 production company Cruydt-hoeck (Groningen, The Netherlands), that grows plants originating from
185 field-collected seeds, delivered the seeds for *G. pyrenaicum*. For all plant species, the seeds were
186 surface-sterilized by washing for 3 min in a 10% bleach solution, followed by rinsing with
187 demineralized water, after which they were germinated on glass beads. After 20 days, the seedlings
188 were collected for LAESI analysis.

189 **LAESI mass spectrometry imaging**

190 The LAESI-MSI of intact roots collected from the seedlings was carried out on a Protea Biosciences
191 DP-1000 LAESI system (Protea Bioscience Inc., Morgantown) coupled to a Waters model Synapt G2S
192 (Waters Corporation) mass spectrometer. The LAESI system was equipped with a 2940-nm mid-
193 infrared laser yielding a spot size of 200 μm . The laser was set to fire 10 times per x-y location (spot)
194 at a frequency of 10 Hz and 100% output energy. The system was set to shoot at 105 locations per
195 plant root (grid of 21 x 5 positions). A syringe pump was delivering the solvent mixture of
196 methanol/water/formic-acid (50:50:0.1% v/v) at 2 $\mu\text{L}/\text{min}$ to a PicoTip (5cm x 100 μm diameter)
197 stainless steel nanospray emitter operating in positive ion mode at 3800 V. The LAESI was operated
198 using LAESI Desktop Software V2.0.1.3 (Protea Biosciences Inc.). The Time of Flight (TOF) mass

199 analyzer of the Synapt G2S was operated in V-reflectron mode at a mass resolution of 18.000 to
200 20.000. The source temperature was 150 °C, and the sampling cone voltage was 30 V. The data was
201 acquired in a mass range of m/z 50 to 1200. The acquired MS data was lock mass corrected post data
202 acquisition using leucine enkephalin ($C_{28}H_{37}N_5O_7$, $m/z = 556.2771$), which was added in the spray as
203 an internal standard.

204 **Data processing, peak-detection and chemometrics**

205 All the acquired Waters .raw data files were first pre-processed to remove noise and to make the data
206 comparable. Since the root samples used in this study were tiny, many LAESI ablation spots
207 constituted the background on which the root samples were placed. In order to avoid including the
208 mass spectra purely consisting of spectral signals from the background, 50 ablation spots per sample
209 replicate, present on the root section were selected manually. The selected ablation spots for every
210 sample replicate are displayed in **Supplementary Figure 1**. The mass spectra arising from the spots
211 colored in green are included in the study whereas those in red have been excluded.

212 The spectra from all the 50 selected spots for each replicate were averaged. Processing of
213 these mass spectra involved multiple steps. An overview of the data processing steps applied is
214 provided in **Figure 5**. First, square root transformation was applied to overcome the dependency of
215 variance on the mean. Then, baseline correction was performed to enhance the contrast of peaks to
216 the baseline. For better comparison of intensity values and to remove small batch effects, Total-Ion-
217 Current (TIC)-based normalization was applied. This was followed by spectral alignment and peak
218 detection to extract a list of significant mass features for each sample replicate. In the end, a mass
219 feature matrix was generated with sample replicates in columns and mass features in rows. This
220 feature matrix was used to perform chemometric analysis. The preprocessing and peak-detection
221 steps were applied using R scripts developed in-house and the functions available within the
222 MALDIquant R package [20].

223 To perform multivariate analysis, the feature matrix was imported into Metaboanalyst 3.0 [21].
224 Principal component analysis (PCA), was initially applied to visualize the intrinsic spectral differences
225 in the non-native, range-expanding plant species and congeneric native plant species. In order to get
226 an overview of the differences amongst the samples, a dendrogram showing clustering of the sample
227 replicates was generated, using the Euclidean distance measure and the Ward's clustering algorithm.

228 To visualize the number of differential metabolites in in non-native, range-expanding plant species and
229 congeneric native plant species, a pairwise comparative analysis was performed. To graphically
230 illustrate these differences volcano plots were generated. Metabolites with a fold change (FC)
231 threshold of 2 on the x-axis and a t-tests threshold (p-value) of 0.1 on the y-axis were considered
232 significant. Box plots for selected significant metabolites were created to display changes in the
233 concentration of native and range-expanding species. Corresponding accurate ion intensity maps (± 1
234 ppm) displaying spatial distribution for these selected mass features were created using the ProteaPlot
235 software V2.0.1.3 (Protea Biosciences Inc., Morgantown, WV). Venn diagrams were drawn using the
236 jvenn tool [22] to plot the number of shared and unique metabolites for each pair of samples.

237 **AVAILABILITY OF SOURCE CODE AND REQUIREMENTS**

238 Project name: LAESI-MSI-Root-Metabolomics

239 Project home page: <https://github.com/purvakulkarni7/LAESI-MSI-Root-Metabolomics>

240 Operating system(s): platform independent

241 Programming language: R

242 Other requirements: R ($\geq 3.2.0$), MALDIquant package, MALDIquantForeign package

243 License: GNU General Public License version 2.0 (GPLv2).

244 Any restrictions to use by non-academics: none

245 **ABBREVIATIONS**

246 MS: mass spectrometry; MSI: mass spectrometry imaging; LAESI: laser-assisted electrospray
247 ionization; CJ: *Centaurea jacea* L.; CS: *Centaurea stoebe* L.; GM: *Geranium molle* L.; GP: *Geranium*
248 *pyrenaicum* Burm.; *m/z*: mass by charge; GC: gas chromatography; TOF: Time-of-flight; PCA:
249 principal component analysis; PC: principal component; FC: fold change.

250 **ACKNOWLEDGEMENTS**

251 We thank Frank Claassen from the department of Agrotechnology and Food Sciences at the
252 Wageningen University for assistance with LAESI-MSI measurement and Julio Pereira da Silva for
253 help with the experimental preparation. Purva Kulkarni is supported by the strategic project fund from

254 the Netherlands Institute of Ecology (NIOO-KNAW). Rutger A. Wilschut and Wim H. van der Putten
255 are supported by the ERC advanced grant ERC-Adv 26055290. This is publication XXX of the
256 Netherlands Institute of Ecology (NIOO-KNAW).

257 **COMPETING FINANCIAL INTERESTS**

258 The authors declare that they have no competing interests.

259 **AUTHOR CONTRIBUTIONS**

260 P.G., K.J.F.V. and R.A.W. devised the project. P.G. and R.A.W. oversaw the sample collection and the
261 data acquisition. P.K. planned and performed the bioinformatics analysis, interpretation of results and
262 prepared the figures. P.K., R.A.W. and P.G. wrote the manuscript. W.H.v.d.P., P.G., K.J.F.V. and
263 R.A.W. provided their comment and contributed to substantial revision of the manuscript.

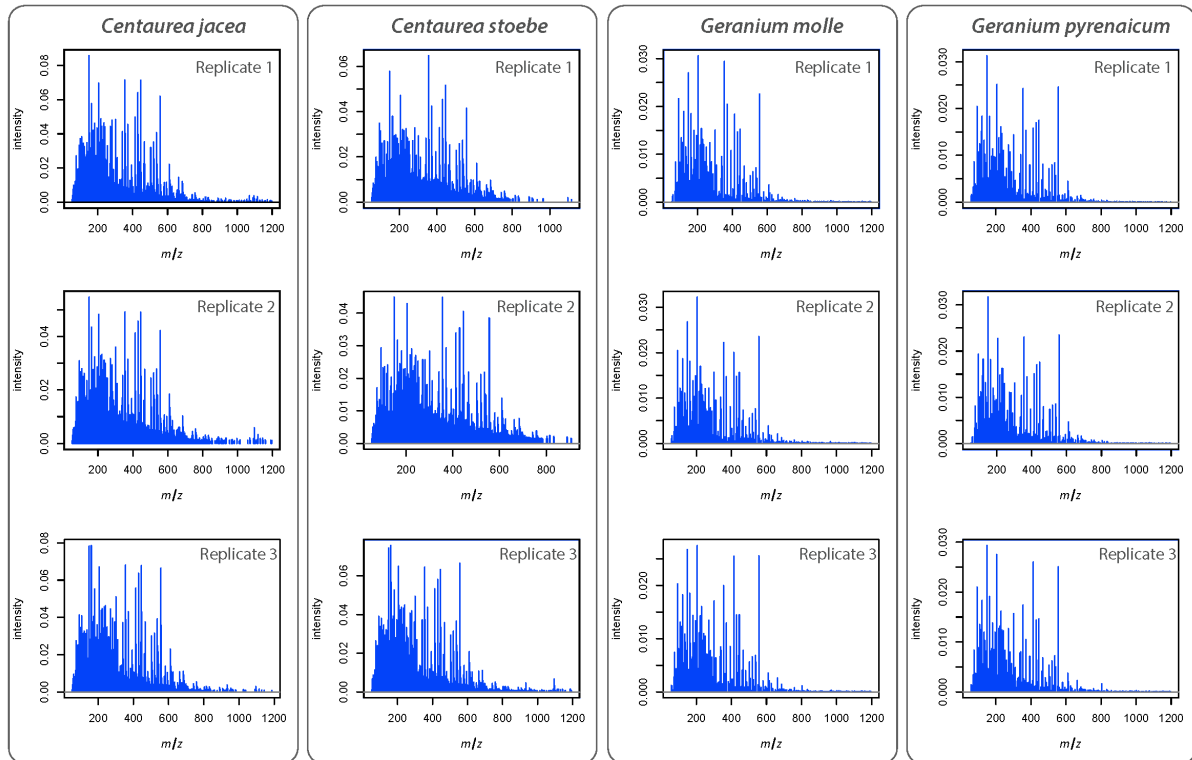
264 **REFERENCES**

- 265 1. Petras D, Jarmusch AK, Dorrestein PC. From single cells to our planet—recent advances in using mass
266 spectrometry for spatially resolved metabolomics. *Curr. Opin. Chem. Biol.* Elsevier Current Trends; 2017, p. 24–
267 31.
- 268 2. Wu C, Dill AL, Eberlin LS, Cooks RG, Ifa DR. Mass spectrometry imaging under ambient conditions. *Mass*
269 *Spectrom Rev.* Wiley Subscription Services, Inc., A Wiley Company; 2013; 32:218–43.
- 270 3. Cooks RG, Ouyang Z, Takats Z, Wiseman JM. Detection Technologies. *Ambient mass spectrometry.* Science.
271 American Association for the Advancement of Science; 2006; 311:1566–70.
- 272 4. Nemes P, Vertes A. Laser ablation electrospray ionization for atmospheric pressure, in vivo, and imaging mass
273 spectrometry. *Anal Chem.* American Chemical Society; 2007; 79:8098–106.
- 274 5. Chen Z, Vertes A. Early plume expansion in atmospheric pressure midinfrared laser ablation of water-rich
275 targets. *Phys Rev E.* American Physical Society; 2008; 77:36316.
- 276 6. Chen Z, Bogaerts A, Vertes A. Phase explosion in atmospheric pressure infrared laser ablation from water-rich
277 targets. *Appl Phys Lett.* American Institute of Physics; 2006; 89:41503.
- 278 7. Bjarnholt N, Li B, D’Alvise J, Janfelt C. Mass spectrometry imaging of plant metabolites—principles and
279 possibilities. *Nat Prod Rep.* 2014;31:818–37.
- 280 8. Shrestha B, Vertes A. In Situ Metabolic Profiling of Single Cells by Laser Ablation Electrospray Ionization Mass
281 Spectrometry. *Anal Chem.* American Chemical Society; 2009; 81:8265–71.

- 282 9. Walther G-R, Post E, Convey P, Menzel A, Parmesan C, Beebee TJC, et al. Ecological responses to recent
283 climate change. *Nature*. Nature Publishing Group; 2002; 416:389–95.
- 284 10. Le Roux PC, McGeoch MA. Rapid range expansion and community reorganization in response to warming.
285 *Glob Chang Biol*. Blackwell Publishing Ltd; 2008; 14:2950–62.
- 286 11. Cappuccino N, Arnason JT. Novel chemistry of invasive exotic plants. *Biol Lett*. The Royal Society; 2006;
287 2:189–93.
- 288 12. Callaway RM, Aschehoug ET. Invasive plants versus their new and old neighbors: a mechanism for exotic
289 invasion. *Science*. 2000; 290:521–3.
- 290 13. Marler MJ, Zabinski CA, Callaway RM. Mycorrhizae indirectly enhance competitive effects of an invasive forb
291 on native bunchgrass. *Ecology*. Ecological Society of America; 1999; 80:1180–6.
- 292 14. Stinson KA, Campbell SA, Powell JR, Wolfe BE, Callaway RM, Thelen GC, et al. Invasive Plant Suppresses
293 the Growth of Native Tree Seedlings by Disrupting Belowground Mutualisms. *PLoS Biol*. Public Library of
294 Science; 2006; 4:e140.
- 295 15. Schaffner U, Ridenour WM, Wolf VC, Bassett T, Müller C, Müller-Schärer H, et al. Plant invasions, generalist
296 herbivores, and novel defense weapons. *Ecology*. 2011; 92:829–35.
- 297 16. Macel M, de Vos RCH, Jansen JJ, van der Putten WH, van Dam NM. Novel chemistry of invasive plants:
298 exotic species have more unique metabolomic profiles than native congeners. *Ecol Evol*. Wiley-Blackwell; 2014;
299 4:2777–86.
- 300 17. Senior JK, Potts BM, Davies NW, Wooliver RC, Schweitzer JA, Bailey JK, et al. Phylogeny Explains Variation
301 in The Root Chemistry of Eucalyptus Species. *J Chem Ecol*. 2016; 42:1086–97.
- 302 18. Wilschut RA, Silva JCP, Garbeva P, van der Putten WH. Belowground Plant–Herbivore Interactions Vary
303 among Climate-Driven Range-Expanding Plant Species with Different Degrees of Novel Chemistry. *Front Plant*
304 *Sci*. *Frontiers*; 2017; 8:1861.
- 305 19. Callaway RM, Ridenour WM. Novel weapons: invasive success and the evolution of increased competitive
306 ability. *Front Ecol Environ*. Wiley-Blackwell; 2004;2:436–43.
- 307 20. Gibb S, Strimmer K. MALDIquant: a versatile R package for the analysis of mass spectrometry data.
308 *Bioinformatics*. 2012; 28:2270–1.
- 309 21. Xia J, Sinelnikov I V., Han B, Wishart DS. MetaboAnalyst 3.0—making metabolomics more meaningful.
310 *Nucleic Acids Res*. Oxford University Press; 2015; 43:W251–7.

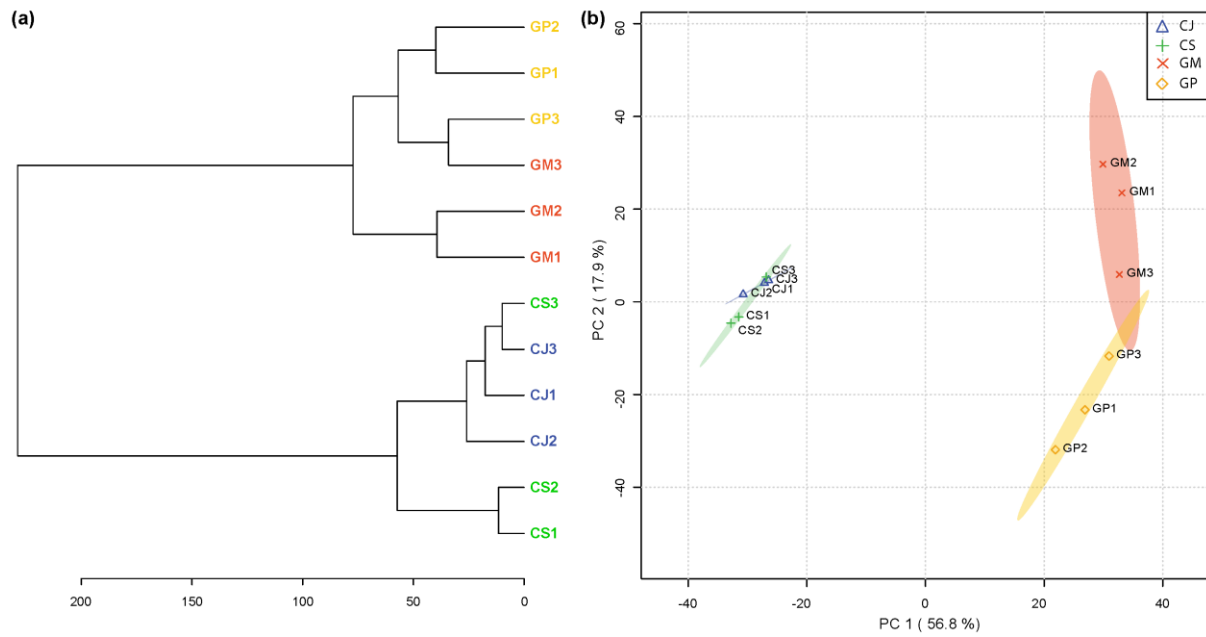
311 22. Bardou P, Mariette J, Escudié F, Djemiel C, Klopp C. jvenn: an interactive Venn diagram viewer. BMC
312 Bioinformatics. BioMed Central; 2014; 15:293.

313 **FIGURE CAPTIONS**

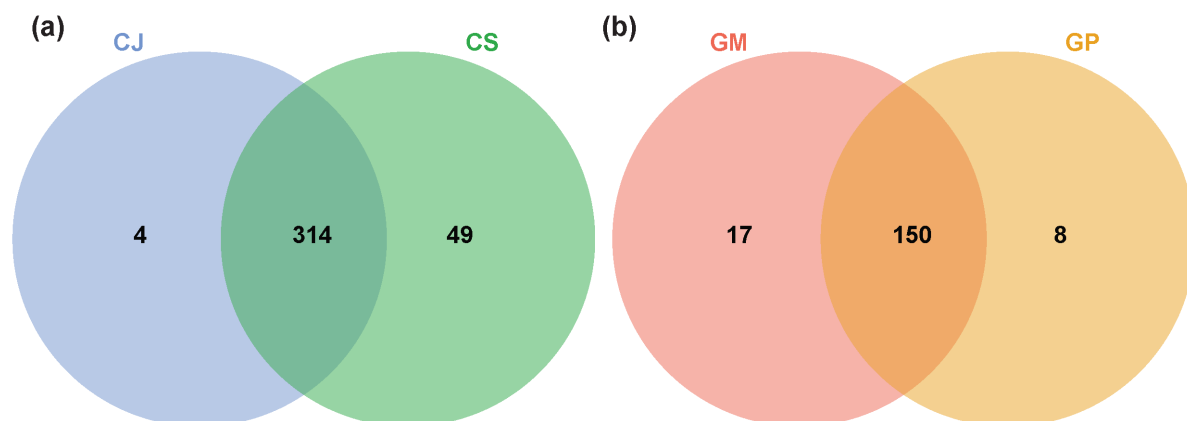


314 **Figure 1: Metabolic profiling and comparison of LAESI-MS spectra from native and range**
315 **expanding plant species.** Each representative mass spectra is generated by averaging and

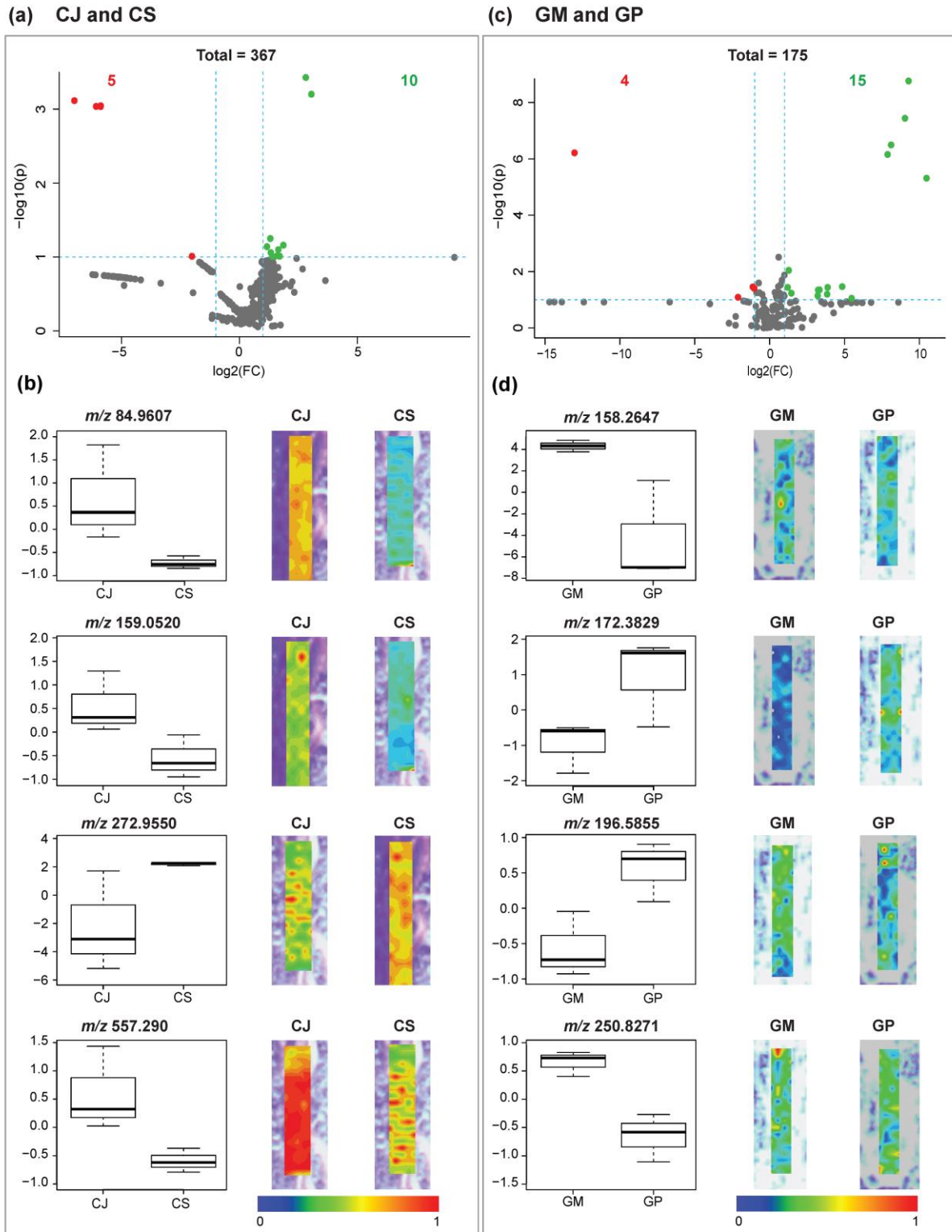
316 preprocessing the signals acquired in positive ion mode, arising from the 50 ablation spots present on
317 the imaged root sample for each replicate. The averaged preprocessed mass spectra are displayed for
318 the three replicates of native species (*C. jacea* and *G. molle*) and the three replicates for range
319 expanding plant species (*C. stoebe* L. and *G. pyrenaicum*).
320



321
322 **Figure 2: Heat map with dendrogram and Principal component analysis (PCA) score plot for the**
323 **selected native and range expanding species. (a)** Species clustering represented as a dendrogram
324 (distance measure used is Euclidean and clustering algorithm is ward). Each node in the dendrogram
325 corresponds to a single replicate belonging either to the range-expanding or to the congeneric native
326 plant species. **(b)** The PCA score plot displays the total explained variance of >70 % for component 1
327 and component 2. Ovals represent 95% confidence intervals. Each oval represents a sample group
328 and each point represents a single sample.

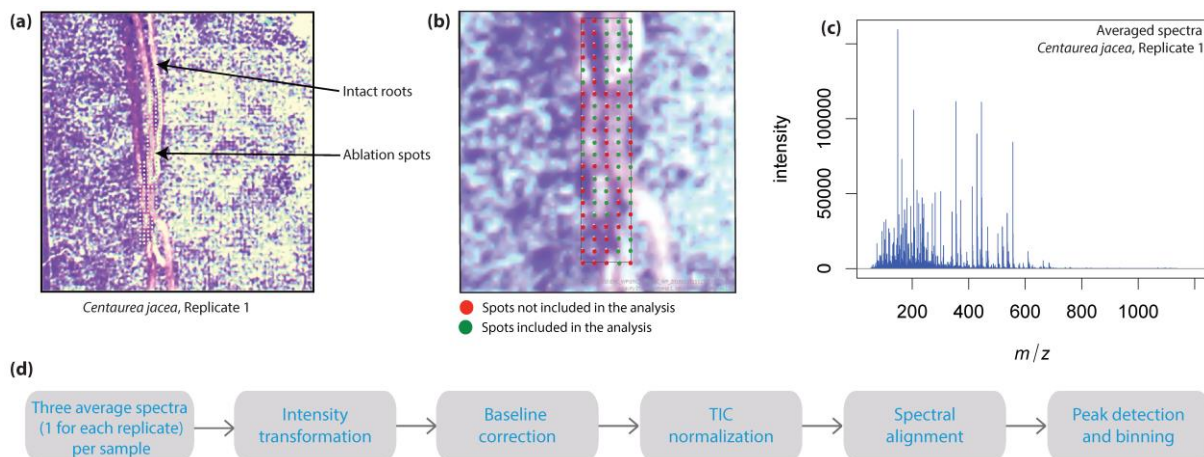


329
330 **Figure 3: Venn diagram showing overlapping and unique metabolites associated with native**
331 **and range expanding plant species. (a)** Venn diagram for *C. jacea* (CJ) and *C. stoebe* (CS).
332 **(b)** Venn diagram for *G. molle* (GM) and *G. pyrenaicum* (GP). To construct the Venn
333 diagram, a single mass feature was considered even if it was present in only one replicate for
334 a specific sample species.



335
336 **Figure 4: Volcano plots and box plots to demonstrate metabolite concentration differences**
337 **observed in native and range expanding plant species. (a) Volcano plot for *C. jacea* (CJ) vs. *C.***
338 ***stoebe* (CS). (b) Volcano plot for *G. molle* (GM) vs. *G. pyrenaicum* (GP). Each point in the volcano plot**
339 **represents one metabolite. Significant metabolites were calculated with a fold change (FC) threshold**
340 **of 2 on the x-axis and a t-tests threshold of 0.1 on the y-axis. The red and the green dots indicate**

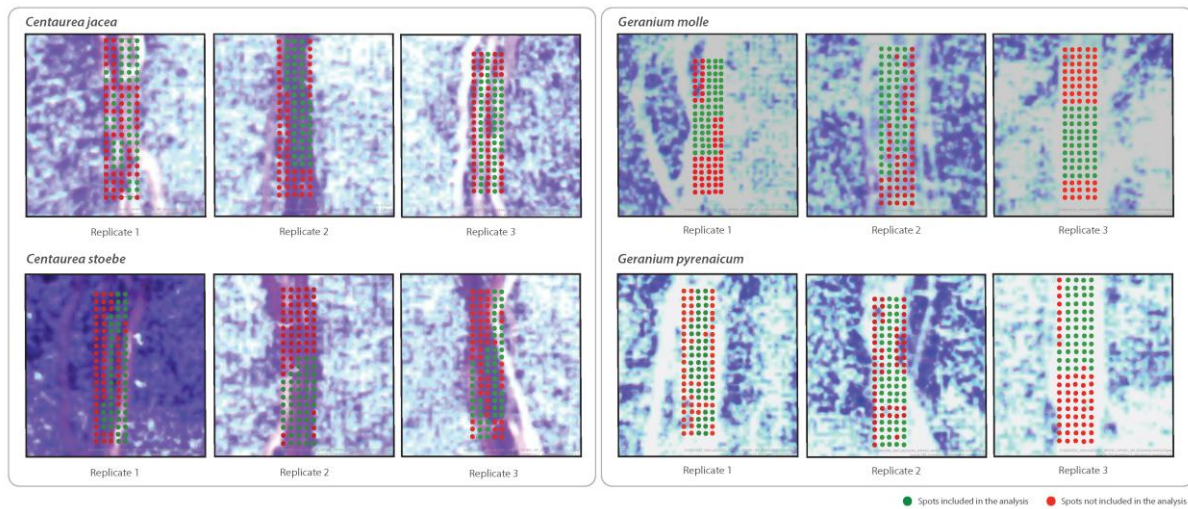
341 statistically significant metabolites, and the gray dots below the FC threshold line represent statistically
342 non-significant metabolites. The vertical FC threshold lines indicates an increase or decrease in
343 concentration of metabolites. Negative \log_2 (FC) values indicated in red represent lower
344 concentrations in native than in range expanding species; positive values indicated in green represent
345 higher concentrations of metabolites in native than in range expanding species. The box plots for the
346 detected metabolites and their corresponding ion intensity maps below each volcano plot display the
347 localization of the selected metabolites that are significantly different in the respective native and
348 range expanding species. The signal intensity in the ion intensity maps are represented in rainbow
349 color scale, in a mass window of ± 1 mDa.



350
351 **Figure 5: Data preparation and processing steps applied post acquisition. (a)** Optical image for
352 the intact roots of a single replicate of *C. jacea* with labeled ablation spots. **(b)** Ablation spots present
353 on the root selected (in green) for further analysis. **(c)** Averaged spectra acquired from all the 50
354 selected spots per replicate. **(d)** Data pre-processing and peak-detection steps applied to all spectra
355 for a sample.

356

357 **SUPPLEMENTARY FIGURE**



358
359 **Supplementary Figure 1: Ablation spots present on the imaged root samples selected for**
360 **further analysis.** A set of 50 ablation spots for each replicate of the native and range expanding
361 species was selected. The spots selected for further analysis are shown in green. These are present
362 on the root sample that has been imaged. The spots that are not selected for further analysis are
363 displayed in red. These may or may not arise from the imaged root samples.

364

365 **TABLES**

366 **Table 1:** Overview of the number of metabolites detected in each sample replicate after preprocessing
 367 and peak detection of the acquired LAESI-MSI datasets.

| Replicate | <i>C. jacea</i> (CJ) | <i>C. stoebe</i> (CS) | <i>G. molle</i> (GM) | <i>G. pyrenaicum</i> (GP) |
|-----------|----------------------|-----------------------|----------------------|---------------------------|
| 1 | 283 | 332 | 143 | 129 |
| 2 | 204 | 301 | 151 | 127 |
| 3 | 286 | 286 | 131 | 122 |

368

369 **SUPPLEMENTARY TABLE**

370 **Supplementary Table 1:** Significant metabolites and their respective fold change ($\log_2(\text{FC})$) and p
 371 values ($-\log_{10}(p)$) for native and range expanding pairs *C. jacea* (CJ) vs. *C. stoebe* (CS) and *G. molle*
 372 (*GM*) vs. *G. pyrenaicum* (GP).

373

| CJ vs. CS | | | GM vs. GP | | |
|------------|---------------------|-----------------|------------|---------------------|-----------------|
| <i>m/z</i> | $\log_2(\text{FC})$ | $-\log_{10}(p)$ | <i>m/z</i> | $\log_2(\text{FC})$ | $-\log_{10}(p)$ |
| 892.2366 | 2.8154 | 3.4282 | 887.111 | 9.2804 | 8.7636 |
| 837.1989 | 3.0537 | 3.2022 | 885.1207 | 9.039 | 7.44 |
| 245.094 | -7.0019 | 3.1155 | 980.8683 | 8.1151 | 6.4941 |
| 270.964 | -5.8824 | 3.0457 | 486.52534 | -13.033 | 6.2126 |
| 213.12 | -6.0788 | 3.037 | 1096.874 | 7.8812 | 6.1562 |
| 352.952 | -5.8897 | 3.0347 | 492.5648 | 10.482 | 5.3132 |
| 557.2904 | 1.3107 | 1.2492 | 250.8271 | 1.2766 | 2.0428 |
| 136.0762 | 1.8652 | 1.1594 | 158.2647 | 4.8462 | 1.4655 |
| 159.0517 | 1.1667 | 1.1396 | 196.58554 | -1.1204 | 1.455 |
| 84.96074 | 1.65 | 1.0988 | 252.3956 | 1.2045 | 1.4386 |
| 536.1757 | 1.3311 | 1.0584 | 1142.875 | 3.8741 | 1.4379 |
| 99.00528 | 1.6044 | 1.0152 | 64.50864 | -1.0269 | 1.4038 |
| 87.0236 | 1.7072 | 1.0096 | 922.8092 | 3.3317 | 1.3522 |
| 272.955 | -2.013 | 1.0087 | 1024.339 | 3.2395 | 1.3445 |
| 59.02047 | 1.4073 | 1.0044 | 637.3655 | 1.4521 | 1.2323 |
| | | | 187.6822 | 3.8414 | 1.1946 |
| | | | 92.45683 | 3.2114 | 1.1408 |
| | | | 172.38286 | -2.1105 | 1.0878 |
| | | | 859.1226 | 5.4774 | 1.0524 |